

# Gas Hydrate Phase Equilibrium in Methane + Ethylene Glycol, Diethylene Glycol, or Triethylene Glycol + Water System

Amir H. Mohammadi\* and Dominique Richon

MINES ParisTech, CEP/TEP - Centre Énergétique et Procédés, 35 Rue Saint Honoré, 77305 Fontainebleau, France

**ABSTRACT:** In this communication, experimental hydrate dissociation pressures for the methane + diethylene glycol + water and methane + triethylene glycol + water systems are reported at 0.2, 0.35, and 0.5 mass fractions of glycol in aqueous solution in the temperature ranges of (265.0 to 283.2) K and (266.3 to 284.6) K, respectively. We also report experimental hydrate dissociation pressures for the methane + ethylene glycol (EG) + water system at a mass fraction of ethylene glycol of 0.65 in aqueous solution in the temperature range of (247.4 to 250.7) K. The experimental data were generated using an isochoric pressure-search method. The experimental hydrate dissociation data are compared with the corresponding literature data and also the literature data in the presence of pure water as well as the predictions of a thermodynamic model (HWHYD model). It is found that the experimental hydrate dissociation data reported in the literature for the aforementioned systems are rare. A discussion is made on the reliability of the literature data and also the predictions of the thermodynamic model.

## 1. INTRODUCTION

Gas hydrates or clathrate hydrates are ice-like crystalline solids, in which small molecules (typically gases) are trapped inside cages of hydrogen bonded water molecules. The formation of gas hydrates can give rise to equipment blockages, operational problems, and safety concerns in hydrocarbon production, transportation, and processing.<sup>1</sup> Organic inhibitors like methanol or ethylene glycol (EG) are normally used to avoid the formation of gas hydrates.<sup>1</sup> Reliable gas hydrate phase equilibrium data for the main components of these fluids in the presence/absence of inhibitor aqueous solutions are required to develop and validate thermodynamic models for predicting hydrate stability zones of hydrocarbon fluids.<sup>1</sup> Although sufficient experimental data have been reported for gas hydrates of these components at low glycol mass fractions in aqueous solution,<sup>1</sup> information for gas hydrates of main components of hydrocarbon fluids at high glycol mass fractions in aqueous solution is limited.<sup>1</sup>

In this communication, experimental hydrate dissociation pressures for methane + diethylene glycol (DEG) + water and methane + triethylene glycol (TEG) + water systems are reported at 0.2, 0.35, and 0.5 mass fractions of glycol in aqueous solution in the temperature ranges of (265.0 to 283.2) K and (266.3 to 284.6) K, respectively. We also report experimental hydrate dissociation pressures for the methane + ethylene glycol + water system at 0.65 mass fractions of ethylene glycol in aqueous solution in the temperature range of (247.4 to 250.7) K. The experimental data were measured using an isochoric pressure-search method.<sup>2–5</sup> Comparisons are made between our experimental dissociation data with the corresponding literature data<sup>5–11</sup> and the experimental hydrate dissociation data in the presence of pure water<sup>12–14</sup> as well as the predictions of a thermodynamic model (HWHYD model).<sup>15</sup> The reliability of the experimental hydrate dissociation data reported in the literature as well as the predictions of the model is discussed.

## 2. EXPERIMENTAL SECTION

**2.1. Materials.** Table 1 reports the purities and supplier names of the materials used in this work. Aqueous solutions were prepared following the gravimetric method using an accurate analytical balance (mass uncertainty  $\pm 0.0001$  g). Consequently, uncertainties on the basis of mole fraction are estimated to be less than 0.01.

**2.2. Experimental Apparatus.** The schematic diagram of this apparatus is given in Figure 1. Briefly, the main part of the apparatus is a cylindrical vessel made of Hastelloy, which can withstand pressures up to 20 MPa. The volume of the vessel is 30 cm<sup>3</sup>. A stirrer installed in the vessel agitates the fluids and the hydrate crystals. Two platinum resistance thermometers (Pt100) inserted into the vessel were used to measure temperatures and check with temperature measurement uncertainty, which is estimated to be less than 0.1 K. This temperature uncertainty estimation comes from calibration against a 25  $\Omega$  reference platinum resistance thermometer. The pressure in the

**Table 1. Purities and Suppliers of Materials<sup>a</sup>**

material	supplier	purity
methane	Messer Griesheim	0.99995 (mole fraction)
EG	Aldrich	0.99 (GC)
DEG	Sigma-Aldrich	0.99 (GC)
TEG	Aldrich	0.99 (GC)

<sup>a</sup> Deionized water was used in all experiments.

**Special Issue:** Kenneth N. Marsh Festschrift

**Received:** May 24, 2011

**Accepted:** July 26, 2011

**Published:** September 13, 2011

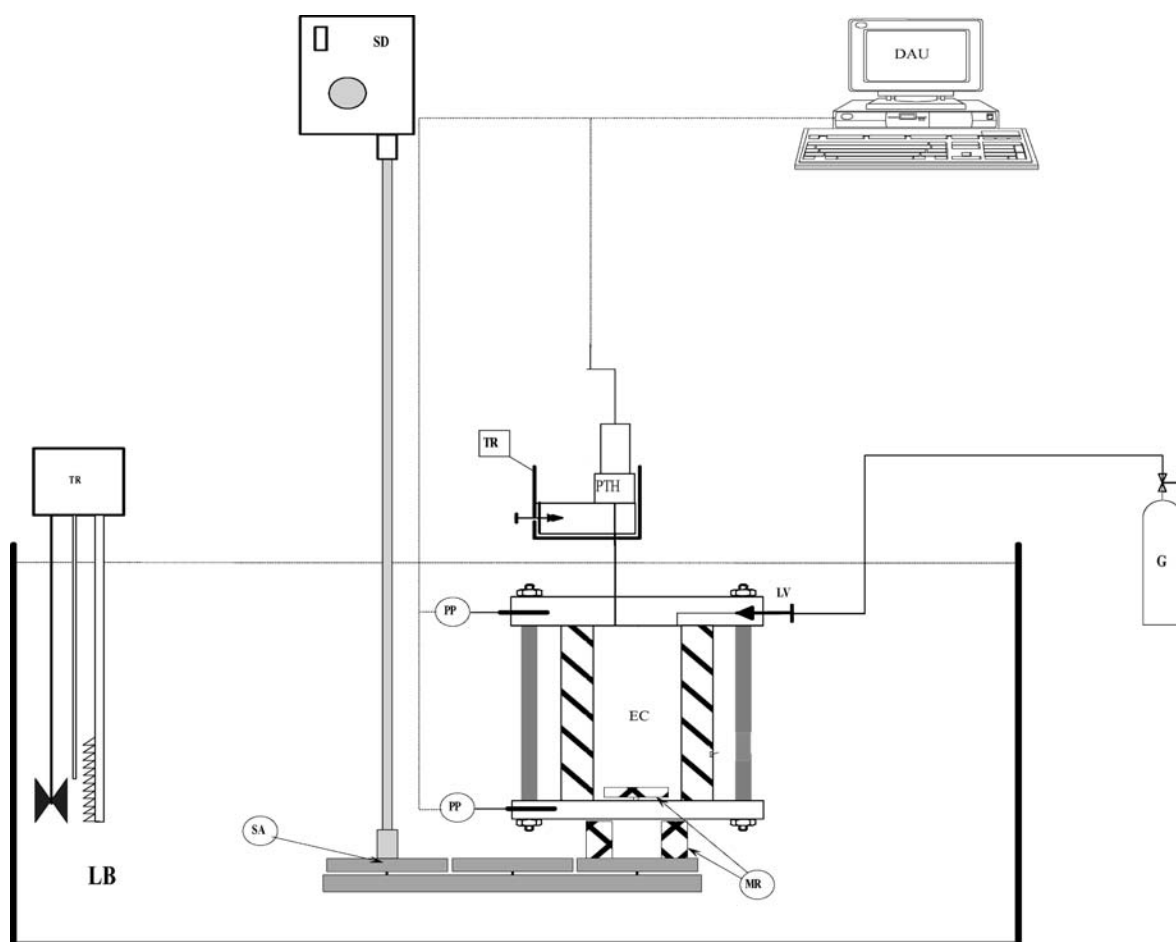


**Figure 1.** Schematic diagram of the experimental apparatus. DAU, data acquisition unit; EC, equilibrium cell; G, gas cylinder; LB, liquid bath; LV, loading valve; MR, magnetic rod; PP, platinum probe (temperature sensor); PTH, pressure transducer; SA, stirring assembly; SD, stirring device with a variable speed motor; TR, temperature controller (regulator).

vessel was measured with a DRUCK pressure transducer (Druck, type PTX611) calibrated for pressure ranges up to 16 MPa. The pressure measurement uncertainty was estimated to be less than 5 kPa, as a result of calibration against a dead weight balance (Desgranges and Huot, model 520).

**2.3. Experimental Method.** The hydrate dissociation conditions were measured with an isochoric pressure search method.<sup>2–5</sup> The reliability of this method has already been examined and reported<sup>16,17</sup> and is similar to the method of Ohmura and colleagues.<sup>18</sup> The vessel containing aqueous solution (approximately 10 % by volume of the vessel is filled with aqueous solution) is immersed into the temperature-controlled bath, and the gas is supplied from a cylinder through a pressure-regulating valve into the vessel. Note that the vessel is evacuated before introduction of any aqueous solution and gas. After obtaining temperature and pressure stability (far enough from the hydrate formation region), the valve in the line connecting the vessel and the cylinder is closed. Subsequently, the temperature is slowly decreased to form the hydrate. Hydrate formation in the vessel is observed when a pressure drop at constant temperature is detected by the data acquisition unit.<sup>18</sup> The temperature is then increased with steps of 0.1 K.<sup>18</sup> At every temperature step, the temperature is kept constant with enough time to obtain an equilibrium state in the equilibrium cell.<sup>18</sup> Therefore, a pressure–temperature diagram is sketched for each experimental run, from

which we determine the hydrate dissociation point.<sup>18</sup> During the dissociation of the hydrate crystals inside hydrate formation region, the pressure is gradually increased by increasing the temperature.<sup>18</sup> However, outside this region, a slighter pressure increase is observed during the increase of temperature.<sup>18</sup> Consequently, the real hydrate dissociation point can be determined when the slope of the pressure–temperature diagram changes suddenly.<sup>18</sup> The uncertainties for the hydrate dissociation temperatures and pressures are expected to be  $\pm 0.1$  K and  $\pm 0.03$  MPa.

### 3. RESULTS AND DISCUSSION

Tables 2 to 4 and Figures 2 to 4 report all of the dissociation data. A semilogarithmic scale has been used in these figures to show the data consistency, as the logarithm of hydrate dissociation pressure versus temperature has approximately linear behavior.<sup>1</sup> In these figures, we have shown the corresponding literature data<sup>5–11</sup> as well as some selected experimental data from the literature on the dissociation conditions of methane hydrates in the presence of pure water<sup>12–14</sup> to show the inhibition effects of the aqueous solutions studied in this work. Note that the inhibition effect means shifting hydrate dissociation conditions to high pressures/low temperatures due to the presence of inhibitor in aqueous solution. The predictions of the

**Table 2. Experimental Hydrate Dissociation Conditions for the Methane + EG + Water System<sup>a</sup>**

T/K	p/MPa
247.4	10.38
248.8	12.82
250.7	18.32

<sup>a</sup>The concentration of ethylene glycol in aqueous solution is 0.65 mass fraction.

**Table 3. Experimental Hydrate Dissociation Conditions for the Methane + DEG + Water System<sup>a</sup>**

T/K	p/MPa
<i>w</i> = 0.20	
276.4	5.22
277.3	5.69
280.1	7.68
282.0	9.49
283.2	10.71
<i>w</i> = 0.35	
271.3	4.94
273.2	6.01
275.5	7.67
277.1	9.21
279.0	11.55
<i>w</i> = 0.50	
265.0	6.15
266.7	7.22
269.2	9.18
271.3	11.90
272.8	14.50

<sup>a</sup>*w* represents the mass fraction of inhibitor in aqueous solution.

HWHYD thermodynamic model<sup>15</sup> have also been shown in these figures. Briefly, the model<sup>15</sup> is based on the equality of fugacity concept, which uses the Valderrama modification of the Patel–Teja equation of state<sup>19</sup> and non-density dependent mixing rules<sup>20</sup> for modeling the fluid phases, while the van der Waals and Platteeuw theory<sup>21</sup> is used for modeling the hydrate phase. As can be observed in the figures, this model cannot reliably predict the hydrate dissociation conditions in the presence of aqueous solutions of the investigated glycols. Particularly, it fails for the DEG and TEG containing systems. For the EG containing systems, it can predict only the conditions of low concentrations of EG aqueous solutions as shown in Figure 2. The latter figure also shows the experimental hydrate dissociation data for the methane + EG + water systems up to 0.50 mass fraction of EG aqueous solutions reported already by these authors as well as 0.65 mass fraction of EG aqueous solutions measured in this work. As can be seen in this figure, the agreement between the literature data is generally satisfactory. Figure 3 clearly shows some disagreements in the literature data. For instance, the experimental data reported in ref 9 for 0.09989 mass fraction DEG aqueous solution overlap the literature data in the presence of water. Furthermore, the latter data show less inhibition effects than the experimental data reported in ref 8 for 0.066 mass fraction DEG aqueous solution. On the other hand,

**Table 4. Experimental Hydrate Dissociation Conditions for the Methane + TEG + Water System<sup>a</sup>**

T/K	p/MPa
<i>w</i> = 0.20	
275.7	4.64
278.8	6.31
280.6	7.68
282.5	9.51
284.6	11.92
<i>w</i> = 0.35	
273.6	5.23
275.7	6.49
277.5	7.88
279.4	9.68
280.5	10.95
<i>w</i> = 0.50	
266.3	5.50
268.8	7.05
270.5	8.25
272.5	10.11
274.2	12.52

<sup>a</sup>*w* represents the mass fraction of inhibitor in aqueous solution.

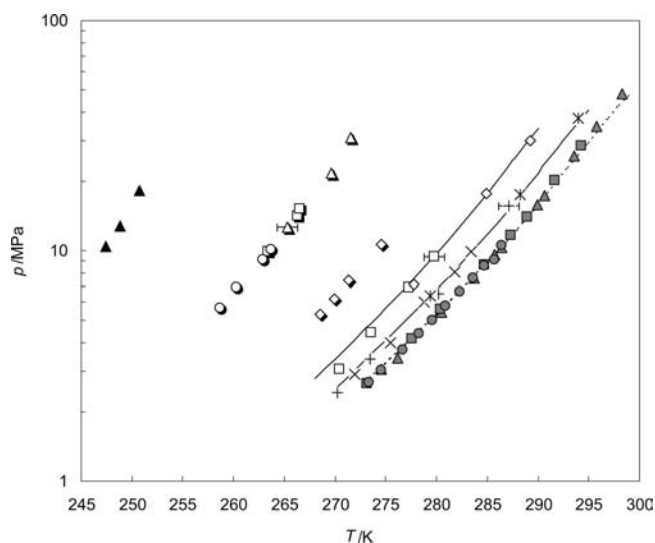


**Figure 2.** Experimental and predicted hydrate dissociation conditions for the methane + EG + water system. Symbols represent experimental dissociation conditions. Curves represent predictions of the thermodynamic model.<sup>15</sup> *w* represents the mass fraction of inhibitor in aqueous solution. Methane + water system: ▲ (gray), ref 11; ● (gray), ref 12; ■ (gray), ref 13. Methane + EG + water system: ×, *w* = 0.1, ref 5; \*, *w* = 0.1, ref 6; +, *w* = 0.1, ref 7; □, *w* = 0.2, ref 5; ◇, *w* = 0.2, ref 6; ○ (shadow), *w* = 0.35, ref 5; □ (shadow), *w* = 0.5, ref 5; △ (shadow), *w* = 0.5, ref 6; □ (shadow), *w* = 0.5, ref 6; ▲, *w* = 0.65, this work. Dashed curve: thermodynamic model<sup>15</sup> predictions for the methane + water system. Solid curve: thermodynamic model<sup>15</sup> predictions for the methane + EG + water system. Temperature error band: 1 K.

the experimental data reported in ref 9 for 0.2494 mass fraction DEG aqueous solution show a similar hydrate inhibition effect as our experimental data for 0.20 mass fraction DEG aqueous

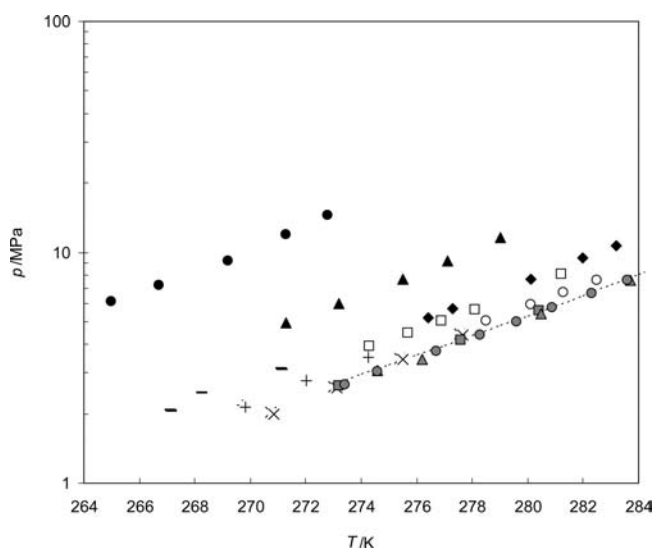


**Figure 3.** Experimental and predicted hydrate dissociation conditions for the methane + DEG + water system. Symbols represent experimental dissociation conditions. The curve represents predictions of the thermodynamic model.<sup>15</sup>  $w$  represents the mass fraction of inhibitor in aqueous solution. Methane + water system:  $\blacktriangle$  (gray), ref 11;  $\bullet$  (gray), ref 12;  $\blacksquare$  (gray), ref 13. Methane + DEG + water system:  $\circ$ ,  $w = 0.066$ , ref 8;  $\times$ ,  $w = 0.09989$ , ref 9;  $+$ ,  $w = 0.1499$ , ref 9;  $\square$ ,  $w = 0.168$ , ref 8;  $\blacklozenge$ ,  $w = 0.20$ , this work;  $-$ ,  $w = 0.2494$ , ref 9;  $\blacktriangle$ ,  $w = 0.35$ , this work;  $\bullet$ ,  $w = 0.50$ , this work. Dashed curve: thermodynamic model<sup>15</sup> predictions for the methane + water system.

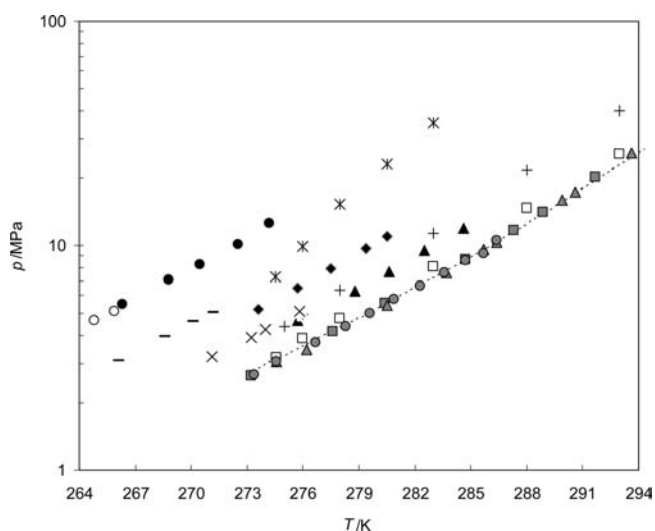


**Figure 4.** Experimental and predicted hydrate dissociation conditions for the methane + TEG + water system. Symbols represent experimental dissociation conditions. The curve represents predictions of the thermodynamic model.<sup>15</sup>  $w$  represents the mass fraction of inhibitor in aqueous solution. Methane + water system:  $\blacktriangle$  (gray), ref 11;  $\bullet$  (gray), ref 12;  $\blacksquare$  (gray), ref 13. Methane + TEG + water system:  $\square$ ,  $w = 0.10$ , ref 11;  $\blacktriangle$ ,  $w = 0.20$ , this work;  $+$ ,  $w = 0.20$ , ref 11;  $\times$ ,  $w = 0.245$ , ref 10;  $\blacklozenge$ ,  $w = 0.35$ , this work;  $-$ ,  $w = 0.40$ , ref 10;  $*$ ,  $w = 0.40$ , ref 11;  $\circ$ ,  $w = 0.50$ , ref 10;  $\bullet$ ,  $w = 0.50$ , this work.

solution. In overall, the hydrate dissociation data reported in ref 9 for the methane + DEG + water systems seem to be unreliable. In Figure 4, it is clear that the hydrate dissociation data reported in ref 11 for the methane + TEG + water system at 0.40 mass

fraction TEG aqueous solution are not reliable. Similarly, the experimental data of ref 11 for 0.20 mass fraction TEG aqueous solution are not in agreement with our experimental data.

#### 4. CONCLUSIONS

Experimental hydrate dissociation data are reported for methane + DEG + water and methane + TEG + water systems at 0.2, 0.35, and 0.5 mass fractions of glycol in aqueous solution in the temperature ranges of (265.0 to 283.2) K and (266.3 to 284.6) K, respectively. We also report experimental hydrate dissociation pressures for the methane + ethylene glycol + water system at 0.65 mass fractions of ethylene glycol in aqueous solution in the temperature range of (247.4 to 250.7) K. An isochoric pressure-search method<sup>2–5</sup> was used for performing all of the measurements. It is found that the hydrate dissociation data at high concentrations of glycol in aqueous solution are rare. Moreover, some disagreements in the literature data for the hydrate dissociation conditions of the methane + DEG + water and methane + TEG + water systems are observed. The predictions of the HWHYD thermodynamic model<sup>15</sup> for the studied systems are generally unreliable.

#### AUTHOR INFORMATION

##### Corresponding Author

\*E-mail: amir-hossein.mohammadi@ensmp.fr. Tel.: +(33) 1 64 69 49 70. Fax: +(33) 1 64 69 49 68.

#### REFERENCES

- (1) Sloan, E. D.; Koh, C. A. *Clathrate Hydrates of Natural Gases*, 3rd ed.; CRC Press: Boca Raton, FL, 2008.
- (2) Mohammadi, A. H.; Richon, D. Equilibrium Data of Carbonyl Sulfide and Hydrogen Sulfide Clathrate Hydrates. *J. Chem. Eng. Data* **2009**, *54*, 2338–2340.
- (3) Mohammadi, A. H.; Kraoui, I.; Richon, D. Methane hydrate phase equilibrium in the presence of NaBr, KBr, CaBr<sub>2</sub>, K<sub>2</sub>CO<sub>3</sub>, and MgCl<sub>2</sub> aqueous solutions: Experimental measurements and predictions of dissociation conditions. *J. Chem. Thermodyn.* **2009**, *41*, 779–782.
- (4) Tohidi, B.; Burgass, R. W.; Danesh, A.; Østergaard, K. K.; Todd, A. C. Improving the Accuracy of Gas Hydrate Dissociation Point Measurements. *Ann. N.Y. Acad. Sci.* **2000**, *912*, 924–931.
- (5) Mohammadi, A. H.; Richon, D. Phase Equilibria of Methane Hydrates in the Presence of Methanol and/or Ethylene Glycol Aqueous Solutions. *Ind. Eng. Chem. Res.* **2010**, *49*, 925–928.
- (6) Haghghi, H.; Chapoy, A.; Burgess, R.; Tohidi, B. Experimental and thermodynamic modelling of systems containing water and ethylene glycol: Application to flow assurance and gas processing. *Fluid Phase Equilib.* **2009**, *276*, 24–30.
- (7) Robinson, D. B.; Ng, H. J. Hydrate Formation and Inhibition in Gas or Gas Condensate Streams. *J. Can. Petrol. Technol.* Jul-Aug **1986**, *25/4*, quoted in ref 1.
- (8) Afzal, W.; Mohammadi, A. H.; Richon, D. Experimental Measurements and Predictions of Dissociation Conditions for Methane, Ethane, Propane, and Carbon Dioxide Simple Hydrates in the Presence of Diethylene Glycol Aqueous Solutions. *J. Chem. Eng. Data* **2008**, *53*, 663–666.
- (9) Mahmoodaghdam, E.; Bishnoi, P. R. Equilibrium Data for Methane, Ethane, and Propane Incipient Hydrate Formation in Aqueous Solutions of Ethylene Glycol and Diethylene Glycol. *J. Chem. Eng. Data* **2002**, *47*, 278–281.
- (10) Afzal, W.; Mohammadi, A. H.; Richon, D. Experimental Measurements and Predictions of Dissociation Conditions for Carbon Dioxide and Methane Hydrates in the Presence Triethylene Glycol Aqueous Solutions. *J. Chem. Eng. Data* **2007**, *52*, 2053–2055.

(11) Ross, M. J.; Toczylkin, L. S. Hydrate Dissociation Pressures for Methane or Ethane in the Presence of Aqueous Solutions of Triethylene Glycol. *J. Chem. Eng. Data* **1992**, *37*, 488–491.

(12) Mohammadi, A. H.; Anderson, R.; Tohidi, B. Carbon Monoxide Clathrate Hydrates: Equilibrium Data and Thermodynamic Modeling. *AIChE J.* **2005**, *51*, 2825–2833; quoted in ref 1.

(13) Adisasmito, S.; Frank, R. J.; Sloan, E. D. Hydrates of carbon dioxide and methane mixtures. *J. Chem. Eng. Data* **1991**, *36*, 68–71; quoted in ref 1.

(14) Jhaveri, J.; Robinson, D. B. Hydrates in the methane-nitrogen system. *Can. J. Chem. Eng.* **1965**, *43*, 75–78; quoted in ref 1.

(15) HWHYD Heriot-Watt University Hydrate model (Version 1.1). <http://www.pet.hw.ac.uk/research/hydrate/> (Accessed June 2007).

(16) Mohammadi, A. H.; Eslamimanesh, A.; Belandria, V.; Richon, D. Phase Equilibria of Semi-Clathrate Hydrates of CO<sub>2</sub>, N<sub>2</sub>, CH<sub>4</sub>, or H<sub>2</sub> + Tetra-n-butylammonium Bromide Aqueous Solution. *J. Chem. Eng. Data* **2011**, DOI: 10.1021/je2005159.

(17) Semi-Clathrate Hydrate Phase Equilibrium Measurements for CO<sub>2</sub> + N<sub>2</sub> + Tetra-n-Butylammonium Bromide Aqueous Solutions. Private communication, **2011**.

(18) Ohmura, R.; Takeya, S.; Uchida, T.; Ebinuma, T. Clathrate hydrate formed with methane and 2-Propanol: Confirmation of structure II hydrate formation. *Ind. Eng. Chem. Res.* **2004**, *43*, 4964–4966.

(19) Valderrama, J. O. A generalized Patel-Teja equation of state for polar and nonpolar fluids and their mixtures. *J. Chem. Eng. Jpn.* **1990**, *23*, 87–91.

(20) Avlonitis, D.; Danesh, A.; Todd, A. C. Equilibrium data and thermodynamic modelling of cyclohexane gas hydrates. *Fluid Phase Equilib.* **1994**, *94*, 181–216.

(21) van der Waals, J. H.; Platteeuw, J. C. Clathrate Solutions. *Adv. Chem. Phys.* **1959**, *2*, 1–57; quoted in ref 1.